

Geophysical Research Letters

RESEARCH LETTER

10.1029/2019GL084470

Special Section:

Bridging Weather and Climate:
Subseasonal-to-Seasonal (S2S)
Prediction

Key Points:

- Tornado frequencies during the last half of May 2019 were over three times the climatological average
- This extended period of favorable tornado conditions were successfully forecast nearly 4 weeks in advance
- Changes in atmospheric angular momentum associated tropical convection appear to have created this forecast of opportunity

Correspondence to:
V. A. Gensini,
vgensini@niu.edu

Citation:
Gensini, V. A., Gold, D., Allen, J. T., & Barrett, B. S. (2019). Extended U.S. tornado outbreak during late May 2019: A forecast of opportunity. *Geophysical Research Letters*, 46. <https://doi.org/10.1029/2019GL084470>

Received 8 JUL 2019
Accepted 1 AUG 2019

©2019. The Authors.

This is an open access article under the terms of the Creative Commons Attribution-NonCommercial-NoDerivs License, which permits use and distribution in any medium, provided the original work is properly cited, the use is non-commercial and no modifications or adaptations are made.

Extended U.S. Tornado Outbreak During Late May 2019: A Forecast of Opportunity

Vittorio A. Gensini¹ , David Gold² , John T. Allen³ , and Bradford S. Barrett⁴ 

¹Department of Geographic and Atmospheric Sciences, Northern Illinois University, DeKalb, IL, USA, ²IBM, Global Business Services, Weather Analytics Center of Competency, Armonk, NY, USA, ³Department of Earth and Atmospheric Science, Central Michigan University, Mount Pleasant, MI, USA, ⁴Oceanography Department, United States Naval Academy, Annapolis, MD, USA

Abstract The second half of May 2019 was an unusually active period for tornadic thunderstorms across the U.S. Great Plains, Midwest, and lower Great Lakes. While this period typically coincides with the peak climatological frequency of tornadoes, preliminary reports of tornadoes were over triple the expected 30-year average. Multiple-day outbreaks of tornadoes are not unprecedented in the United States; however, this event was perhaps the first to be forecast at subseasonal lead times (3–4 weeks) by the Extended Range Tornado Activity Forecast team. This forecast of opportunity was driven, in part, by anomalous convective forcing in portions of the tropical Indian and Pacific Oceans, causing subsequent changes in Northern Hemisphere atmospheric angular momentum. This manuscript analyzes the evolution of hemispheric-scale circulation features leading up to the event, examines teleconnection processes known to influence U.S. tornadoes, and provides insights into the forecast process at subseasonal lead times.

1. Introduction

The period 17–29 May 2019 was among the most active periods of severe weather the United States has seen in years. While 2019 data are still preliminary, at least 374 tornadoes occurred during this 13-day stretch, more than tripling the 1986–2018 average for this period of 107. In total, 757 tornado warnings were issued by the National Oceanic and Atmospheric Administration (NOAA)'s National Weather Service, with seven fatalities reported (Figure 1). This late-May period contributed significantly to the second highest monthly (E)F1+ tornado count (220) on record for May since reliable tornado counts began in the early 1950s, behind only May 2003.

The main synoptic-scale driver of this favorable pattern for tornadic storms was a semipermanent upper-level cyclone across the western contiguous United States (CONUS). This western CONUS trough, in tandem with a downstream eastern CONUS ridge, helped sustain southwesterly midtropospheric and upper-tropospheric flow throughout the period of interest. In fact, several days during the outbreak exhibited observed 250-hPa winds at or above 50 m/s. This synoptic weather regime is recognized as one of the most effective at generating supercell thunderstorms, since it often juxtaposes abundant and deep lower-tropospheric moisture from the Gulf of Mexico, strong tropospheric wind shear, and steep midtropospheric lapse rates (Doswell III, 1987; Mercer et al., 2012; Schultz et al., 2014). These atmospheric ingredients are not uncommon in the month of May across the United States. In fact, multiday episodes of tornadoes, such as those of late May 2019, are not unprecedented in U.S. tornado history (e.g., the prolific tornadoes of 3–11 May 2003; Hamill et al., 2005; Trapp, 2014). What made this particular event unique is that the synoptic-scale conditions favorable for tornadic storms were successfully forecast nearly 4 weeks in advance by the Extended Range Tornado Activity Forecast (ERTAF) team. This forecast lead window includes early portions of the subseasonal forecast period (2 weeks to 2 months) and has recently become an important area of focus for research and operations (Robertson et al., 2015; White et al., 2017). The primary goal herein is to analyze the event from a weather-climate linkage perspective, with particular focus on some known indicators of atmospheric variability associated with subseasonal severe weather modulation across the United States. Data and techniques that were leveraged to make such a prediction, which was perhaps the first of its kind for severe convective storms, provided the motivation for this study.

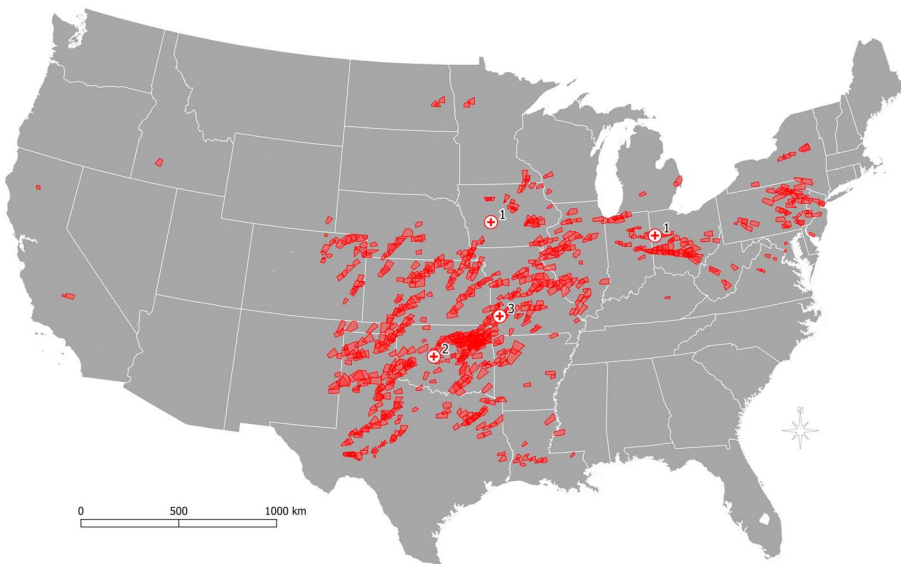


Figure 1. The 757 tornado warnings (red polygons) issued by the National Oceanic and Atmospheric Administration's National Weather Service from 1200 UTC 17 May to 1200 UTC 30 May 2019. Seven fatalities were reported during this period (locations marked by red +).

The leading modes of subseasonal variability associated with U.S. tornadoes are supported by a rapidly growing body of literature. Several studies in recent years have focused on the role of the Madden-Julian Oscillation (MJO; Madden & Julian, 1971) as a driver of tornado and hail activity (Barrett & Gensini, 2013; Barrett & Henley, 2015; Baggett et al., 2018; Thompson & Roundy, 2012; Tippett, 2018) via eastward jet stream extensions and Rossby wave perturbations in response to tropical convection (Moore et al., 2010). Still other studies in recent years have focused on the Global Synoptic Dynamic Model (GSDM; Weickmann & Berry, 2007), which is a dynamical framework underpinned by the Global Wind Oscillation (GWO; Weickmann & Berry, 2009) that considers both the role of tropical variability (including the MJO) and midlatitude processes in modulating severe weather activity (Gensini & Marinaro, 2016; Gensini & Allen, 2018; Moore, 2018).

Results from these works indicate that both MJO and GWO have statistically favorable and unfavorable phases for U.S. tornado and hail frequency. In addition, recurring modes within both oscillations occasionally provide enhanced predictability of future potential for severe weather frequency. Careful monitoring of such oscillations enabled ERTAF forecasters to leverage these signals in real time, allowing for the anticipation of conditions favorable for the extended period of severe weather in May 2019 nearly 4 weeks in advance. This prediction is especially notable given the preseason expectation of below-average frequencies of U.S. tornadoes due to the presence of weak El Niño conditions in the tropical Pacific Ocean (Allen et al., 2015).

The remainder of this article is organized as follows: data used for the analysis are presented in section 2; the subseasonal evolution of different signals that led to the synoptic-scale events of May 2019 is described in section 3; and conclusions from the analysis and discussion of the significance of this event are presented in section 4.

2. Data

Synoptic atmospheric conditions were analyzed using isobaric data from the National Centers for Environmental Prediction/National Center for Atmospheric Research (NCEP/NCAR) reanalysis (Kalnay et al., 1996). Atmospheric angular momentum (AAM) was calculated from the NCEP/NCAR reanalysis using the native T62 Gaussian grid, which has 28 vertical sigma levels. AAM was calculated using 4 times daily averages of zonal wind via the following formula:

$$AAM = \frac{a^3}{g} \int_{-\pi/2}^{\pi/2} \int_0^{2\pi} \int_{p_o}^p \cos^2 \phi d\phi d\lambda u dp \quad (1)$$

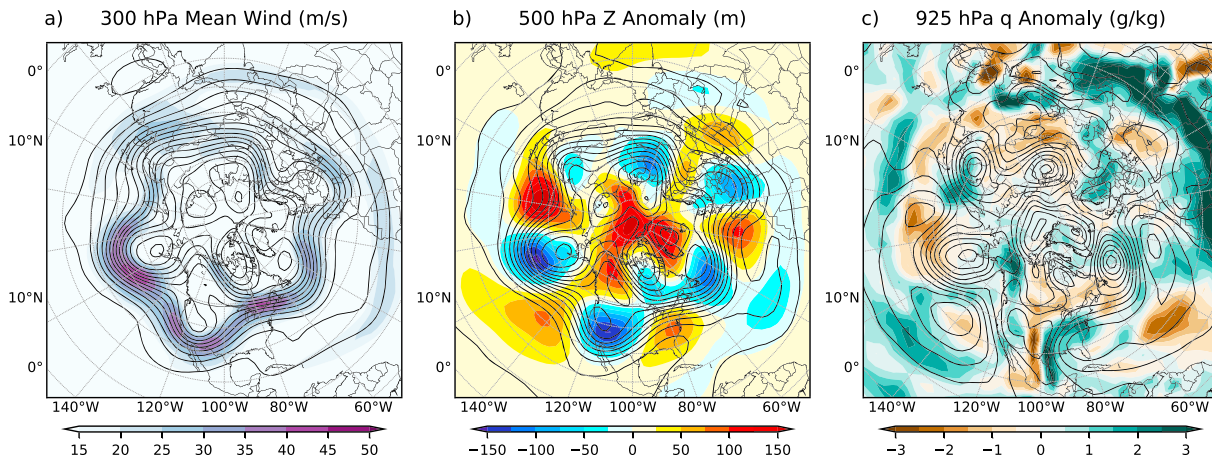


Figure 2. For the period 17–29 May 2019, average (a) 300-hPa wind (m/s) and 300-hPa geopotential height (m), average (b) 500-hPa geopotential height (m) and 500-hPa geopotential height anomaly (m), and average (c) 925-hPa specific humidity anomaly (g/kg) and 925-hPa geopotential height (m) as computed from the National Centers for Environmental Prediction/National Center for Atmospheric Research Reanalysis. Anomalies calculated from the 1980–2010 climatology.

where a is Earth's radius, g is the gravitational constant, ϕ is latitude, λ is longitude, u is zonal wind speed, and p is pressure. AAM tendency was calculated using a fourth-order centered finite difference following Weickmann and Berry (2009). Synoptic anomaly fields were calculated using averages from the 1981–2010 period, and AAM anomalies were calculated using the period 1968–1996. Amplitude and phase of the MJO were obtained from the Australian Bureau of Meteorology (Wheeler & Hendon, 2004) and outgoing longwave radiation was obtained from the NCAR/NOAA interpolated dataset (Liebmann & Smith, 1996). Finally, tornado warnings issued by NOAA's National Weather Service were obtained from the Iowa State University weather warning archive.

3. Results

3.1. Event Summary: Synoptic Pattern

One of the most active periods of severe storms in U.S. history began on 17 May 2019 as a shortwave trough approached the Great Plains from the Great Basin. From 17 May onward, repeated days of severe weather, including several tornado outbreaks (Verbout et al., 2006), occurred as upper-tropospheric southwesterly flow remained persistent over the Great Plains (Figure 2a), with average 300-hPa winds during the period greater than 40 m/s. At 500 hPa, the mean negative geopotential height anomaly for the period was greater than 125 m over a large area covering the western CONUS. A persistent warm sector over the plains was characterized by vertically deep (≥ 2 km above ground level), anomalously rich boundary layer moisture (Figure 2c) and warm temperatures, both of which contributed to moderate-extreme levels of convective available potential energy. In addition, sea surface temperatures in the Gulf of Mexico for the 5-week period leading up to this event were at or above normal, providing a source of boundary layer moisture (Molina & Allen, 2019). Another notable feature of this persistent period of tornado activity was multiple days with relatively weak capping inversions associated with below-average elevated mixed layer temperatures. This promoted high spatial concentrations of severe storms that, given the favorable atmospheric parameters, were able to produce a substantial number of tornadoes.

3.2. Event Evolution: Subseasonal Pattern

ERTAF began in spring 2015 motivated by the realization that patterns favorable for severe weather can sometimes be predicted at extended lead times (7+ days), beyond the typical range at which numerical weather prediction (NWP) models have useful skill at predicting atmospheric ingredients favorable for tornadoes (Gensini & Tippett, 2019; Zhang et al., 2019). These occasional *forecasts of opportunity* are made possible by catching the emergence of coherent subseasonal signals within the GSDM framework and using the time scales typical of these processes to anticipate the development of regional circulation anomalies favorable for tornadoes, such as those that developed in May 2019.

A leading mode of subseasonal variability capable of giving rise to synoptic patterns favorable for enhanced tornadic activity is the MJO (Barrett & Gensini, 2013; Baggett et al., 2018; Thompson & Roundy, 2012;

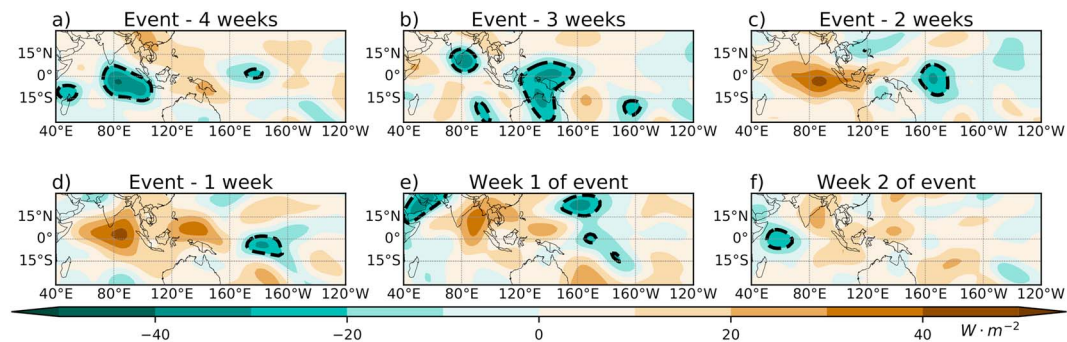


Figure 3. Average weekly OLR anomalies (W/m^2 , color fill) for (a) 19–25 April, (b) 26 April to 2 May, (c) 3–9 May, (d) 10–16 May, (e) 17–23 May, and (f) 24–29 May 2019. Dashed black lines correspond to the $-20 \text{ W}/\text{m}^2$ contour.

Tippett, 2018). As an MJO event evolves over a 40- to 60-day cycle, tropical convection along the equator propagates eastward from the Indian Ocean toward the Pacific. Such propagation was clearly evident in outgoing longwave radiation anomalies (Figure 3) over the 4 weeks leading up to this event. Dynamically, latent heat release results in the formation of an anomalous anticyclone to the northwest of the convection, leading to an intensification of the upper-tropospheric zonal winds to the anticyclone's north (Moore et al., 2010). As the MJO perturbation propagates eastward forcing convection, the net result is an extension of a strong upper-tropospheric jet into the midlatitudes of the central Pacific. When a blocking anticyclone is in place over the eastern North Pacific ocean, this jet extension eventually leads to wave breaking over western North America. It is this wave breaking, and subsequent troughing over the U.S., that links the tropical MJO to U.S. tornado frequency (Barrett & Gensini, 2013; Baggett et al., 2018; Thompson & Roundy, 2012; Tippett, 2018). The predictability of the MJO convection as it moves east from the Indian Ocean across the Pacific Ocean (Lim et al., 2018) allows it to serve as a leading indicator of upcoming tornadic activity once the MJO convection moves into the eastern Pacific Ocean (Baggett et al., 2018).

Multiple time and space scales contribute to subseasonal and low-frequency variability, including El Niño and the MJO. The former was lingering from boreal autumn 2018, while the latter was becoming active from latter April into early May. While El Niño is known to be less favorable to tornado occurrence (Allen et al., 2015; Cook et al., 2017), its modulation of the large-scale circulation is not necessarily unfavorable to tornadic potential. This paradox arises due to its role in the development of a subtropical jet stream over the central and eastern Pacific extending into the Americas. This influence, as illustrated by (Cook et al., 2017) for the later winter months, can be favorable to the development of tornado outbreaks, particularly over the southeastern United States. Indeed, this type of subtropical jet signature was evident in the 4 weeks leading up to the May 2019 event, and the subtropical jet merged with the North Pacific jet for the duration of the event (Figure 4), suggesting that ENSO contributed favorably to this anomalous period of tornado activity.

Four weeks prior to the onset of the extended event, the upper-tropospheric jet structure featured a split pattern, with a maxima over the western Pacific (Figure 4) and a weaker subtropical jet across the Western Hemisphere. By 3 weeks prior to the event (Figure 4b), a Rossby wave train was evolving in the upper troposphere across the Pacific-North America region (Leathers et al., 1991; resembling the negative Pacific-North America pattern identified by Sparrow & Mercer, 2016), while tropical convection had developed into the Maritime Continent and far West Pacific (Figure 3b). The hemispheric pattern at that time was loosely consistent with GSMD Stage 2 (Weickmann & Berry, 2007, cf. Figure 13). Two weeks prior to the event, the Pacific jet further intensified, extending into the central Pacific, consistent with the propagation of the MJO heat source into the equatorial date line region. Simultaneously, the aforementioned Rossby wave train continued to mature and disperse eastward.

By 1 week prior to the event, the north Pacific jet had further intensified and extended across the North Pacific, with wind speeds within the jet for the week of 13–19 May nearly twice the climatological average. The combination of the central Pacific convection, which drove an intensification of the subtropical jet, and the strengthened midlatitude circulation, including blocking in the northeast Pacific, set the stage for wave breaking that subsequently led to a semipersistent CONUS trough. During the first week of the protracted severe weather event, the strong and previously more zonally oriented north Pacific jet transitioned into a meridional configuration associated with persistent western CONUS troughing (Figure 4e). This pattern

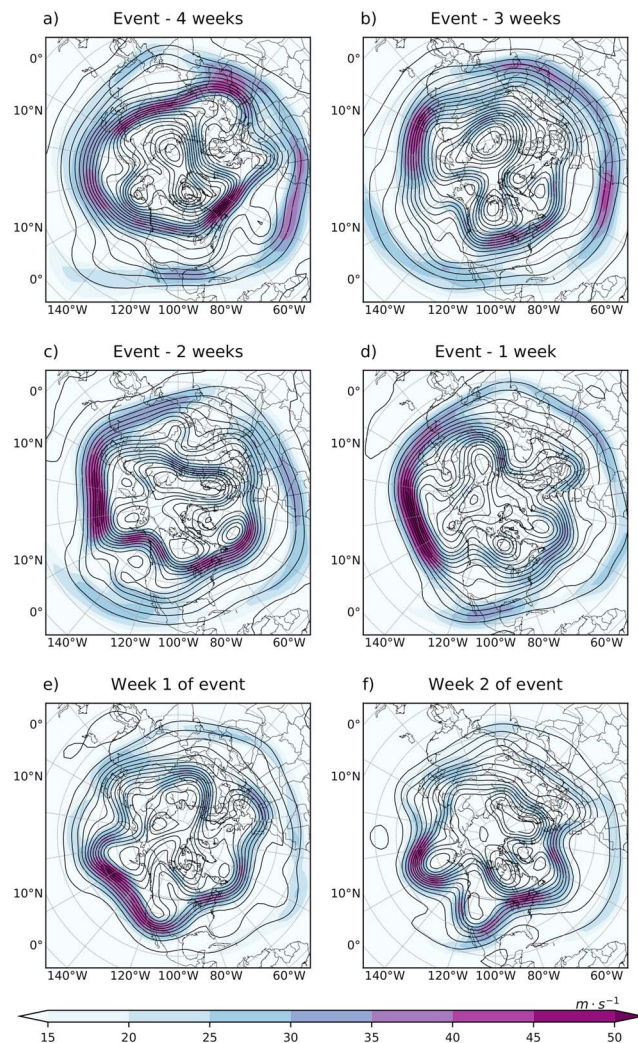


Figure 4. Average 300-hPa geopotential height (contours) and wind speed (color fill) for (a) 19–25 April, (b) 26 April to 2 May, (c) 3–9 May, (d) 10–16 May, (e) 17–23 May, and (f) 24–29 May 2019.

continued into the second week of the event, though with slightly less coupling between the subtropical and midlatitude jet branches (Figure 4f).

3.3. Event Prediction: Attribution to MJO and AAM

By mid-April, ERTAF was looking for catalysts to precipitate the breakdown of the strong Pacific jet (i.e., to facilitate a transition from a more zonal to more meridional orientation), anticipating that the transition would result in an active period of CONUS tornado frequency (Gensini & Marinaro, 2016). The conceptual model that has emerged from Weickmann and Berry (2007) and Weickmann and Berry (2009) provides for a systematic approach to monitoring the time and space scales of the GSDM and GWO that link climate and weather. Indeed, one key link has emerged between tropical modes and midlatitude AAM variability. This framework is particularly amenable to predicting high-impact weather events on subseasonal time scales because the components comprising the GSDM each have distinct characteristic time scales. Furthermore, the framework links the more predictable evolutions in global and zonal mean AAM, as well as the forcings (e.g., mountain and friction torque) of its time tendency, to regional circulation patterns. It is those latter regional variations that are critical to tornado activity, even though they tend to be less predictable by NWP on subseasonal time scales (Weber & Mass, 2019).

In an operational forecast setting, it is possible to anticipate high-impact forecasts of opportunity by identifying slow-varying processes involving the forcing and subsequent damping of AAM (involving the mountain and friction torques), including by the MJO, and the regional patterns that transport AAM poleward,

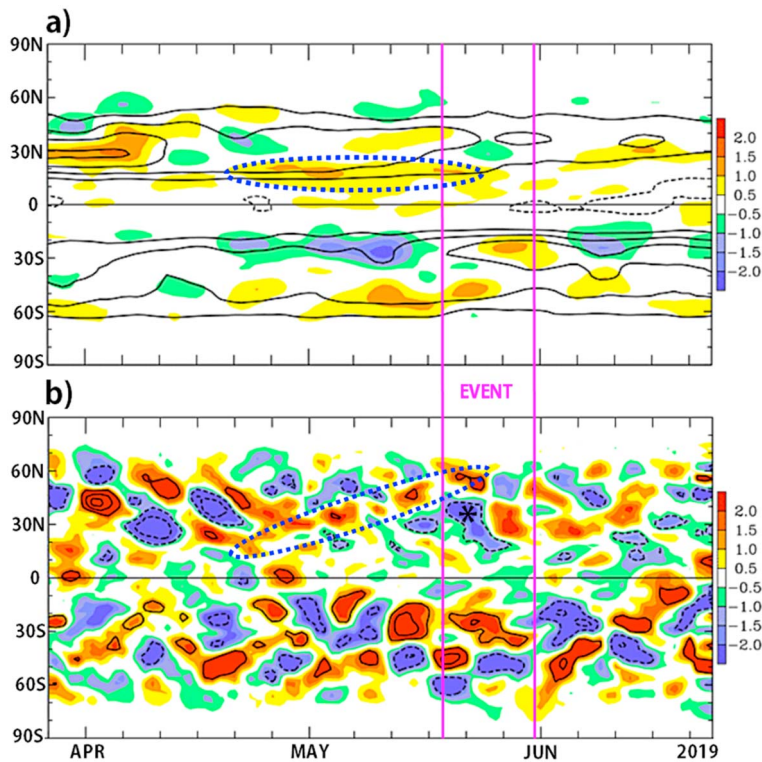


Figure 5. Time-latitude plots of Earth-relative atmospheric angular momentum (a) anomaly (scaled by 10^{24}) and (b) tendency (scaled by 10^{18}). Areas of anomalously high (low) AAM and AAM tendency are shaded using warm (cool) colors. Units are kilograms per square meter per second. AAM = atmospheric angular momentum.

including those that project onto well-known teleconnection patterns (Barnston & Livezey, 1987). Events linking the global and synoptic time and space scales both before and during the 2019 severe weather event were especially well depicted by time-latitude plots of zonally and vertically integrated Earth-relative AAM anomalies (Figure 5a) and their daily tendencies (Figure 5b). Anomalously high (low) AAM is typically associated with anomalously strong (weak) zonal mean winds.

For much of April into early May, there was a belt of anomalously strong zonal winds persisting along 20°N (blue dashed oval Figure 5a). This feature was likely related in large part to the ENSO background state, and during this period appears to have caused a buildup of westerly momentum in the subtropical jet stream. By early May, a branch of this anomalous westerly flow began to move poleward and was associated with a concomitant poleward progression of positive tendency anomalies (blue dashed oval on Figure 5b). Such an evolution in the zonal mean often leads to a collapse of the North Pacific jet stream (Jaffe et al., 2011; Winters et al., 2019), leading the ERTAF team to anticipate the removal of large amounts of AAM from the Northern Hemisphere AAM budget. The foregoing zonal mean evolution was subjectively consistent with a transition from GSMD Stages 3 to 4 (see Weickmann & Berry, 2007, cf. Figure 14), during which time the Pacific jet tends to push inland across the western CONUS, leading to high-impact weather there and eastward. A regional jet collapse did indeed occur (black star on Figure 5b), leading to the development of an anomalous upper-level trough in the western CONUS (Figures 4e and 4f) during the second half of May 2019.

The other primary forecast signal that ERTAF forecasters recognized involved the previously discussed tropical convective signals. Given observed evolution of an active MJO from the Indian Ocean to the Maritime Continent (represented as evolving through Phases 2–4 of the Real-time Multivariate MJO index (RMM; Wheeler & Hendon, 2004) in late April, and NWP ensemble forecasts of continued MJO evolution from the Maritime Continent into the western Pacific (RMM phases 5–7), the ERTAF group assessed increased odds for previously split flows across the Pacific to resolve into a unified and zonally extended Pacific jet stream. The active MJO for this event is diagnosed as a counterclockwise orbit through time in RMM phase space (Figure 6).

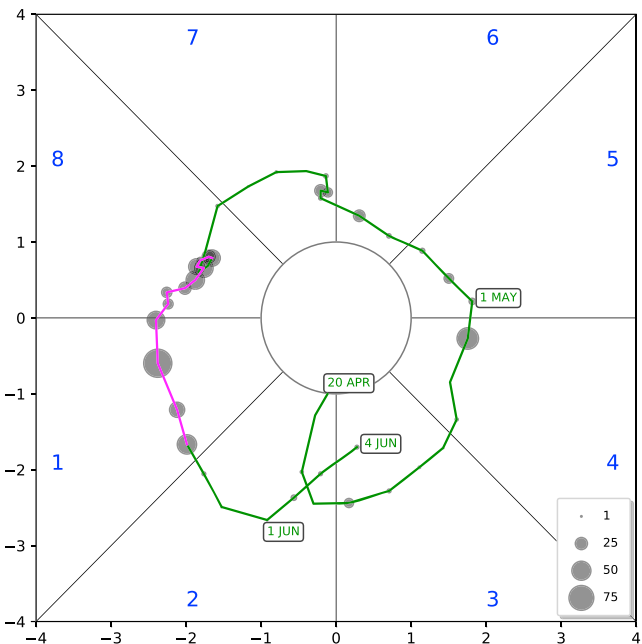


Figure 6. Daily evolution of the MJO via a phase space diagram (RMM1, x axis; RMM2, y axis) from 20 April to 4 June 2019. Magenta line color represents the period 17–29 May. Gray circles represent the number of preliminary tornado reports per respective day. Blue numbers indicate MJO phase. MJO = Madden-Julian Oscillation; RMM = Real-time Multivariate MJO index.

Furthermore, extended-range NWP predictions (e.g., ECMWF ensemble and NOAA's CFSv2) suggested a robust transition in RMM phase space through Phases 8-1-2 during the latter half of May. This transition has been linked to enhanced tornado activity (Barrett & Gensini, 2013; Baggett et al., 2018; Thompson & Roundy, 2012; Tippett, 2018), representing an evolution of the MJO heat source and associated circulation anomalies from the Western Hemisphere back into the Eastern Hemisphere. This is often accompanied by a retraction of the north Pacific jet and formation of a downstream trough over the western CONUS.

Based on these factors, the ERTAF team issued a forecast of “Above Normal” tornado frequency for the U.S. Great Plains eastward into the Midwest and Ohio Valley on 5 May 2019, which was valid for the period 19–25 May 2019. Furthermore, the teams forecast discussion from 28 April 2019 highlighted the likelihood of an active period of severe weather 3–4 weeks into the future. These forecasts likely represent the first successful operational prediction of enhanced CONUS tornado frequency on the subseasonal time scale by leveraging observations, NWP, and recent research findings.

4. Summary and Discussion

The question of why some periods record anomalously above-climatology tornado frequency has troubled many in the U.S. forecasting community for the past few decades (Barrett & Gensini, 2013; Lee et al., 2012; Marzban & Schaefer, 2001; Thompson & Roundy, 2012; Tippett et al., 2015). The period 17–29 May 2019 stands as one of the most active in history, and was characterized by more than three times the climatological number of tornadoes for that time of year, occurring over 13 days and encompassing a wide region of Great Plains and Midwestern CONUS. Here, we have illustrated that a persistent upper-level synoptic trough over the western CONUS, with a downstream ridge aloft over the eastern CONUS, were the main synoptic features of interest. Attribution of such synoptic-scale features to larger-scale, and therefore more predictable signals (Grazzini & Vitart, 2015), remains challenging owing to the complex manner in which processes interact to produce coherent, and therefore potentially predictable, subseasonal evolutions. In the present case, time scales associated with the propagation of the MJO from the equatorial Indian Ocean to the central Pacific Ocean (~20–30 days, or roughly half a cycle) helped create an anomalous North Pacific jet stream extension and retraction sequence that aligned favorably with a transition in AAM from a relatively high to a low state. Previous research indicates that such MJO and AAM/GWO events can lead to favorable atmospheric conditions for tornadic storms in the U.S. Here, with careful monitoring of such features as

they emerged both diagnostically and in NWP-derived RMM phase space, forecasters were able to use signals within both the MJO and AAM/GWO to anticipate the potential for an extended period of favorable severe weather conditions nearly four weeks in advance. While the forecast metric of above-normal, normal, or below-normal (tercile) levels of tornado activity over a subjective spatial region is among the more simple methods available (Klemm & McPherson, 2017; Hartmann et al., 2002), this is a unique example of how understanding tropical convection's role in modulating extratropical dynamic processes can be used to identify a forecast of opportunity for an extreme weather event. The event also offers a pathway for developing operational predictions of U.S. tornado activity across a portion of the subseasonal timescale. Finally, this manuscript represents a single case of a successful subseasonal tornado forecast. More cases, including potential null events, should be examined in future work.

Acknowledgments

The authors wish to acknowledge the pioneering work of Klaus Weickmann and Ed Berry, whose research and contributions more than a decade ago provided the basis for many of the ideas implemented to make the ERTAF project possible. The authors would also like to thank Paul Sirvatka for participation and discussions during the 2019 ERTAF project. MJO data are available for download from the Australian Bureau of Meteorology at <http://www.bom.gov.au/climate/mjo/> website. NCEP/NCAR reanalysis data are available from the Research Data Archive at the National Center for Atmospheric Research, Computational and Information Systems Laboratory (<http://rda.ucar.edu/datasets/ds090.0/>). Archived National Weather Service tornado warnings can be obtained from the Iowa Environmental Mesonet page at <https://mesonet.agron.iastate.edu/request/gis/watchwarn.phpml> website. Patrick Marsh (SPC) provided the preliminary tornado counts for 2019. Two anonymous reviewers provided valuable feedback on an initial draft of this manuscript. Author B. Barrett was partially supported by the Office of Naval Research, award N0001416WX01752.

References

- Allen, J. T., Tippett, M. K., & Sobel, A. H. (2015). Influence of the El Niño–Southern Oscillation on tornado and hail frequency in the United States. *Nature Geoscience*, *8*, 278–283. <https://doi.org/10.1038/ngeo2385>
- Baggett, C. F., Nardi, K. M., Childs, S. J., Zito, S. N., Barnes, E. A., & Maloney, E. D. (2018). Skillful subseasonal forecasts of weekly tornado and hail activity using the Madden-Julian Oscillation. *Journal Geophysical Research: Atmosphere*, *123*, 12,661–12,675. <https://doi.org/10.1029/2018JD029059>
- Barnston, A. G., & Livezey, R. E. (1987). Classification, seasonality and persistence of low-frequency atmospheric circulation patterns. *Monthly Weather Review*, *115*, 1083–1126. [https://doi.org/10.1175/1520-0493\(1987\)115<1083:CSAPOL>2.0.CO;2](https://doi.org/10.1175/1520-0493(1987)115<1083:CSAPOL>2.0.CO;2)
- Barrett, B. S., & Gensini, V. A. (2013). Variability of central United States April–May tornado day likelihood by phase of the Madden-Julian Oscillation. *Geophysical Research Letters*, *40*, 2790–2795. <https://doi.org/10.1002/grl.50522>
- Barrett, B. S., & Henley, B. N. (2015). Intraseasonal variability of hail in the contiguous United States: Relationship to the Madden-Julian Oscillation. *Monthly Weather Review*, *143*(4), 1086–1103. <https://doi.org/10.1175/MWR-D-14-00257.1>
- Cook, A. R., Leslie, L. M., Parsons, D. B., & Schaefer, J. T. (2017). The impact of El Niño–Southern Oscillation (ENSO) on winter and early spring US tornado outbreaks. *Journal of Applied Meteorology and Climatology*, *56*(9), 2455–2478. <https://doi.org/10.1175/JAMC-D-16-0249.1>
- Doswell III, C. A. (1987). The distinction between large-scale and mesoscale contribution to severe convection: A case study example. *Weather Forecasting*, *2*(1), 3–16. [https://doi.org/10.1175/1520-0434\(1987\)002<0003:TDBLSA>2.0.CO;2](https://doi.org/10.1175/1520-0434(1987)002<0003:TDBLSA>2.0.CO;2)
- Gensini, V. A., & Allen, J. T. (2018). U.S. hail frequency and the global wind oscillation. *Geophysical Research Letters*, *45*, 1611–1620. <https://doi.org/10.1029/2017GL076822>
- Gensini, V. A., & Marinaro, A. (2016). Tornado frequency in the United States related to global relative angular momentum. *Monthly Weather Review*, *144*, 801–810. <https://doi.org/10.1175/MWRD-15-0289.1>
- Gensini, V. A., & Tippett, M. K. (2019). Global Ensemble Forecast System (GEFS) predictions of day 1–15 United States tornado and hail frequencies. *Geophysical Research Letter*, *46*, 2922–2930. <https://doi.org/10.1029/2018GL081724>
- Grazzini, F., & Vitart, F. (2015). Atmospheric predictability and Rossby wave packets: Predictability and Rossby wave packets. *Quarterly Journal of the Royal Meteorological Society*, *141*, 2793–2802. <https://doi.org/10.1002/qj.2564>
- Hamill, T. M., Schneider, R. S., Brooks, H. E., Forbes, G. S., Bluestein, H. B., Steinberg, M., et al. (2005). The May 2003 extended tornado outbreak. *Bulletin of the American Meteorological Society*, *86*(4), 531–542. <https://doi.org/10.1175/BAMS-86-4-531>
- Hartmann, H. C., Pagano, T. C., Sorooshian, S., & Bales, R. (2002). Confidence builders: Evaluating seasonal climate forecasts from user perspectives. *Bulletin of the American Meteorological Society*, *83*, 683–698. [https://doi.org/10.1175/1520-0477\(2002\)083<0683:CBESCF>2.3.CO;2](https://doi.org/10.1175/1520-0477(2002)083<0683:CBESCF>2.3.CO;2)
- Jaffe, S. C., Martin, J. E., Vimont, D. J., & Lorenz, D. J. (2011). A synoptic climatology of episodic, subseasonal retractions of the pacific jet. *Journal of Climate*, *24*(11), 2846–2860. <https://doi.org/10.1175/2010JCLI3995.1>
- Kalnay, E., Kanamitsu, M., Kistler, R., Collins, W., Deaven, D., Gandin, L., et al. (1996). The NCEP/NCAR 40-year reanalysis project. *Bulletin of the American Meteorological Society*, *77*(3), 437–472. [https://doi.org/10.1175/1520-0477\(1996\)077<0437:TNYRP>2.0.CO;2](https://doi.org/10.1175/1520-0477(1996)077<0437:TNYRP>2.0.CO;2)
- Klemm, T., & McPherson, R. A. (2017). The development of seasonal climate forecasting for agricultural producers. *Agricultural and Forest Meteorology*, *232*, 384–399. <https://doi.org/10.1016/j.agrformet.2016.09.005>
- Leathers, D. J., Yarnal, B., & Palecki, M. A. (1991). The Pacific/North American teleconnection pattern and United States climate. Part I: Regional temperature and precipitation associations. *Journal of Climate*, *4*(5), 517–528. [https://doi.org/10.1175/1520-0442\(1991\)004<0517:TPATPA>2.0.CO;2](https://doi.org/10.1175/1520-0442(1991)004<0517:TPATPA>2.0.CO;2)
- Lee, S.-K., Atlas, R., Enfield, D., Wang, C., & Liu, H. (2012). Is there an optimal ENSO pattern that enhances large-scale atmospheric processes conducive to tornado outbreaks in the United States? *Journal of Climate*, *26*, 1626–1642. <https://doi.org/10.1175/JCLI-D-12-00128.1>
- Liebmann, B., & Smith, C. A. (1996). Description of a complete (interpolated) outgoing longwave radiation dataset. *Bulletin of the American Meteorological Society*, *77*(6), 1275–1277.
- Lim, Y., Son, S.-W., & Kim, D. (2018). MJO prediction skill of the subseasonal-to-seasonal prediction models. *Journal of Climate*, *31*, 4075–4094. <https://doi.org/10.1175/JCLI-D-17-0545.1>
- Madden, R. A., & Julian, P. R. (1971). Description of global-scale circulation cells in the tropics with a 40–50 day period. *Journal of the Atmospheric Sciences*, *29*, 1107–1123. [https://doi.org/10.1175/1520-0469\(1972\)029<1109:DOGSCC>2.0.CO;2](https://doi.org/10.1175/1520-0469(1972)029<1109:DOGSCC>2.0.CO;2)
- Marzban, C., & Schaefer, J. T. (2001). The correlation between US tornadoes and pacific sea surface temperatures. *Monthly Weather Review*, *129*(4), 884–895. [https://doi.org/10.1175/1520-0493\(2001\)129<0884:TCBUST>2.0.CO;2](https://doi.org/10.1175/1520-0493(2001)129<0884:TCBUST>2.0.CO;2)
- Mercer, A. E., Shafer, C. M., Doswell III, C. A., Leslie, L. M., & Richman, M. B. (2012). Synoptic composites of tornadic and nontornadic outbreaks. *Monthly Weather Review*, *140*, 2590–2608. <https://doi.org/10.1175/MWR-D-12-00029.1>
- Molina, M. J., & Allen, J. T. (2019). On the moisture origins of tornadic thunderstorms. *Journal of Climate*, *32*(14), 4321–4346. <https://doi.org/10.1175/JCLI-D-18-0784.1>
- Moore, T. W. (2018). Annual and seasonal tornado activity in the United States and the global wind oscillation. *Climate Dynamics*, *50*(11–12), 4323–4334.

- Moore, R. W., Martius, O., & Spengler, T. (2010). The modulation of the subtropical and extratropical atmosphere in the Pacific Basin in response to the Madden-Julian Oscillation. *Monthly Weather Review*, 138(7), 2761–2779. <https://doi.org/10.1175/2010mwr3194.1>
- Robertson, A. W., Kumar, A., Peña, M., & Vitart, F. (2015). Improving and promoting subseasonal to seasonal prediction. *Bulletin of the American Meteorological Society*, 96(3), ES49–ES53. <https://doi.org/10.1175/BAMS-D-14-00139.1>
- Schultz, D. M., Richardson, Y. P., Markowski, P. M., & Doswell III, C. A. (2014). Tornadoes in the central United States and the “Clash of Air Masses”. *Bulletin of the American Meteorological Society*, 95(11), 1704–1712. <https://doi.org/10.1175/BAMS-D-13-00252.1>
- Sparrow, K. H., & Mercer, A. E. (2016). Predictability of US tornado outbreak seasons using ENSO and northern hemisphere geopotential height variability. *Geoscience Frontiers*, 7, 21–31. <https://doi.org/10.1016/j.gsf.2015.07.007>
- Thompson, D. B., & Roundy, P. E. (2012). The relationship between the Madden-Julian Oscillation and US violent tornado outbreaks in the spring. *Monthly Weather Review*, 141, 2087–2095. <https://doi.org/10.1175/MWR-D-12-00173.1>
- Tippett, M. K. (2018). Robustness of relations between the MJO and U.S. tornado occurrence. *Monthly Weather Review*, 146(11), 3873–3884. <https://doi.org/10.1175/MWR-D-18-0207.1>
- Tippett, M. K., Allen, J. T., Gensini, V. A., & Brooks, H. E. (2015). Climate and hazardous convective weather. *Current Climate Change Reports*, 1, 60–73. <https://doi.org/10.1007/s40641015-0006-6>
- Trapp, R. J. (2014). On the significance of multiple consecutive days of tornado activity. *Monthly Weather Review*, 142(4), 1452–1459. <https://doi.org/10.1175/MWR-D-13-00347.1>
- Verbout, S. M., Brooks, H. E., Leslie, L. M., & Schultz, D. M. (2006). Evolution of the US Tornado Database: 1954–2003. *Weather Forecasting*, 21, 86–93. <https://doi.org/10.1175/WAF910.1>
- Weber, N. J., & Mass, C. F. (2019). Subseasonal weather prediction in a global convection-permitting model. *Bulletin of the American Meteorological Society*, 100, 1079–1089. <https://doi.org/10.1175/BAMS-D-18-0210.1>
- Weickmann, K., & Berry, E. (2007). A synoptic–dynamic model of subseasonal atmospheric variability. *Monthly Weather Review*, 135(2), 449–474. <https://doi.org/10.1175/MWR3293.1>
- Weickmann, K., & Berry, E. (2009). The tropical Madden-Julian Oscillation and the global wind oscillation. *Monthly Weather Review*, 137(5), 1601–1614. <https://doi.org/10.1175/2008MWR2686.1>
- Wheeler, M. C., & Hendon, H. H. (2004). An all-season real-time multivariate MJO index: Development of an index for monitoring and prediction. *Monthly Weather Review*, 132(8), 1917–1932. [https://doi.org/10.1175/1520-0493\(2004\)132<1917:AARMMI>2.0.CO;2](https://doi.org/10.1175/1520-0493(2004)132<1917:AARMMI>2.0.CO;2)
- White, C. J., Carlsen, H., Robertson, A. W., Klein, R. J., Lazo, J. K., Kumar, A., et al. (2017). Potential applications of subseasonal-to-seasonal (S2S) predictions. *Meteorological Applications*, 24(3), 315–325. <https://doi.org/10.1002/met.1654>
- Winters, A. C., Keyser, D., & Bosart, L. F. (2019). The Development of the North Pacific jet phase diagram as an objective tool to monitor the state and forecast skill of the upper-tropospheric flow pattern. *Weather Forecasting*, 34(1), 199–219. <https://doi.org/10.1175/WAF-D-18-0106.1>
- Zhang, F., Sun, Y. Q., Magnusson, L., Buizza, R., Lin, S.-J., Chen, J.-H., & Emanuel, K. (2019). What is the predictability limit of midlatitude weather? *Journal of the Atmospheric Sciences*, 76(4), 1077–1091. <https://doi.org/10.1175/JAS-D-18-0269.1>